AD NUMBER
AD348709
CLASSIFICATION CHANGES
TO: unclassified
FROM: confidential
LIMITATION CHANGES
TO: Approved for public release, distribution unlimited
FROM: Distribution authorized to DoD only; Administrative/Operational Use; 01 MAR 1964. Other requests shall be referred to Office of Naval Research, ATTN: Code 463, Arlington, VA 22203.
AUTHORITY
31 Mar 1976, DoDD 5200.10; ONR ltr dtd 4 May 1977

AD 348709L

[redacted]

FINAL ENGINEERING REPORT

DOPPLER NAVIGATION STUDY

prepared for

Office of Naval Research

Contract NOnr 3376(00)

1 March 1964

GROUP-4

DOWNGRADED AT 3-YEAR INTERVALS;

DECLASSIFIED AFTER 12 YEARS.

RAYTHEON COMPANY

SUBMARINE SIGNAL DIVISION

Portsmouth, Rhode Island

U.S. military agencies may obtain copies of this report directly from DDC. Other qualified users shall request through the Chief of Naval Research, Code 463.

TABLE OF CONTENTS

Section		Page
1.0	INTRODUCTION	1
2.0	DISCUSSION OF PRINCIPLES AND EXPECTED PERFORMANCE	2
2.1	Doppler Effect	2
2.2	Balanced Acoustic Array	3
2.3	Error-Producing Factors	4
3.0	EXPERIMENTAL RESULTS	20
3.1	Case I - Unbalanced System	20
3.2	Case II - Balanced System	22
3.3	Case III - Velocity-Corrected and Stabilized Balanced System.	23
4.0	EXPERIMENTAL EQUIPMENT	25
4.1	Acoustic Equipment	25
4.2	Mechanical Equipment	26
4.3	Display	29
4.4	Electronics	30
4.5	Significant Equipment Parameters Summarized	31
5.0	CONCLUSIONS.	34
References		35

LIST OF ILLUSTRATIONS

Figure		Page
1	Balanced or 'Janus' Geometry	3
2	Trim Error Geometry	5
3	Error Introduced by Non-Verticality in Janus and Single Systems	6
4	Error in Indicated Distance Travelled Due to Array Vertical Offset	9
5	Doppler Correction By Depression Angle Control	11
6	Compass Error	13
7	Doppler Spectra	16
8	Error Histogram - Case I	21
9	Error Histogram - Case II	24
10	Error Histogram - Case III	24

1.0 INTRODUCTION

This report summarizes the results of the Doppler Navigation Study conducted by the Submarine Signal Division of Raytheon Company for the Office of Naval Research under Contract NOnr 3376(00). The purpose of the study was to establish the feasibility of applying Doppler principle to sonar navigation in shallow depths. The study encompassed both analytic and experimental work, including the fabrication and testing of breadboard circuitry necessary for the experimental phase. The results of the study prove the feasibility of shallow water sonar Doppler navigation.

A system configuration of minimal navigator error is described herein, together with the results of experimental error studies. This study has generated the necessary engineering information for design of a shallow water sonar Doppler navigation system.

2.0 DISCUSSION OF PRINCIPLES AND EXPECTED PERFORMANCE

This section describes the Doppler effect briefly, the geometry of the problem, and other parameters of the experimental apparatus used to validate the analytic results obtained during this study.

2.1 Doppler Effect

The Doppler effect between a moving source/observer and a fixed reflector is accurately described by the following equation:

$$\nu = \frac{2\,V\,f\cos\delta}{C} \Bigg/ \left[1 - \frac{V}{C} - \frac{v_w^2}{C^2} + \frac{v_w V}{C^2}\right] \qquad (2.1.1)$$

where

ν = Doppler shift, cps

V = Ship's horizontal velocity, fps

f = Transmitted frequency, cps

δ = Angle between the acoustic axis and the reflecting surface (depression angle)

C = Velocity of sound in the medium, fps

v_w = Velocity of the medium, fps.

Because of viscous friction on most bottoms, the velocity of the medium at the reflecting surface is usually small and thus may be neglected in the limit, giving

$$\nu = 2Vf\cos\delta/(C - V), \text{ cps} \qquad (2.1.2)$$

For small values of V, relative to C, $C - V_s \approx C$ giving the simplified Doppler equation

$$\nu = \frac{2Vf}{C}\cos\delta, \text{ cps} \qquad (2.1.3)$$

Equation (2.1.3) gives values for ν within 0.5% for V less than 14.3 knots, as compared with Equation (2.1.2).

2.2 Balanced Acoustic Array

In the general sense, the Doppler equation, (2.1.3), is sensitive to any motion relative to the reflecting surface, not only horizontal, but also vertical motion due to bottom slope or ship heave. In order to remove the effects of vertical components, a balanced or 'Janus' system is used. This system is discussed below.

If two acoustic receive-transmit axes (hereafter called acoustic axes) are arranged in a vertical plane as shown in Figure 1, it is easy to show that, as long as the condition of verticality is maintained, the difference of the Doppler shifts of the acoustic axes is insensitive to vertical components of motion.

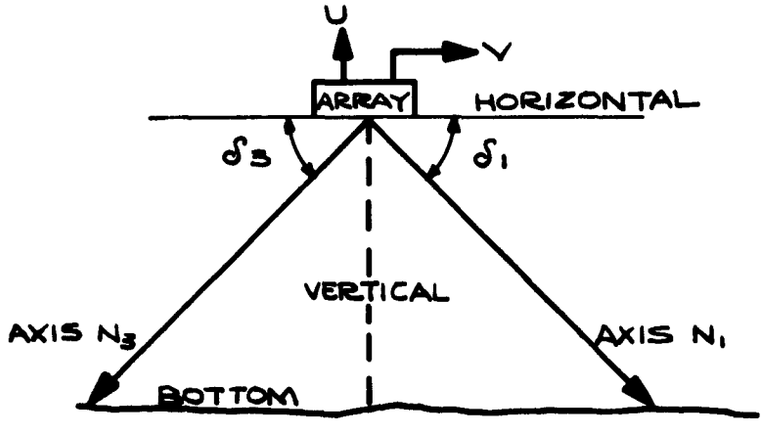

FIGURE 1 BALANCED OR 'JANUS' GEOMETRY

The shift caused by the combined effects of horizontal velocity, V, and vertical velocity, u, along axis N_1 is

$$\nu_1 = (V \cos \delta_1 - u \sin \delta_1) \frac{2f}{C} \qquad (2.2.1)$$

and the shift along N_3 is

$$\nu_3 = -(V \cos \delta_3 + u \sin \delta_3) \frac{2f}{C} \qquad (2.2.2)$$

Substracting (2.2.2) from (2.2.1) with the assumption $\delta_3 = \delta_1$ gives

$$\nu_1 - \nu_3 = \frac{4 V_1 f \cos \delta_3}{C} \qquad (2.2.3)$$

Equation (2.2.3) indicates that the Doppler shift obtained by a balanced system is insensitive to vertical motion and is twice the value of that obtained by horizontal motion of a single axis. It may be said without formal demonstration that these advantages accrue only if the depression angles are equal with respect to the true horizontal, indicating that best accuracy requires that the acoustic axes be space stabilized.

2.3 Error-Producing Factors

Errors accrued in the velocity measuring process can generally be broken down into the categories of 1) Geometry, 2) Medium and 3) Direction. The general geometric parameters can be well-defined, as can the parameters involved in determining direction, but there are certain characteristics of the medium which are not too well-defined at these frequencies.[1]

2.3.1 Vertical Standoff Errors

The errors due to a vertical standoff and/or pitch and roll can be quite easily defined if certain assumptions are made. The following assumptions will be made in this section: 1) No vertical motion effects will be considered, 2) The depression angles in each axis are the same, 3) The separation angles between transducers are exactly 90°, 4) All time-variable effects are symmetrical and occur centrally about the ideal static situation and 5) All static offsets occur in the absence of dynamic variations.

Consider first the static situation where the array vertical has a standoff error with respect to the true vertical, the standoff angle being in the vertical plane containing the depression angles. If the trim angle is θ as shown in Figure 2, the Doppler shifts in the 1 and 3 axes become

$$\nu_1 = K \cos(\delta + \theta) = K \cos\delta(\cos\theta - \tan\delta \sin\theta) \qquad (2.3.1)$$

[1] References will appear on page 35.

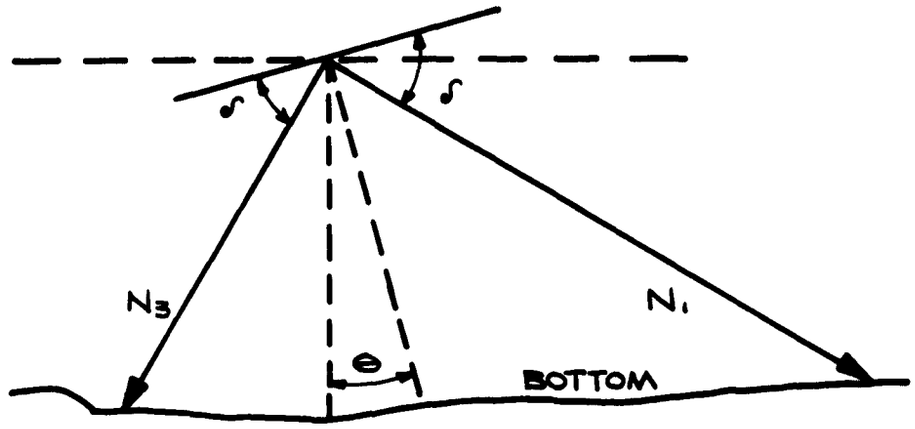

FIGURE 2 TRIM ERROR GEOMETRY

$$\nu_3 = -K \cos(\delta - \theta) = -K \cos\delta (\cos\theta + \tan\delta \sin\theta) \qquad (2.3.2)$$

where

$$K = \frac{2Vf}{C}$$

The error is given as

$$E_1 = 100 (\cos\theta_o - \tan\delta \sin\theta - 1)\% \qquad (2.3.3)$$

for the 1 axis and

$$E_1 = 100 [\cos\theta - (1 + \sin\theta)]\% \qquad (2.3.3a)$$

for $\delta = 45°$.

For the balanced system, the error is

$$E_{13} = -100 (1 - \cos\theta)\% \approx -\frac{100\,\theta^2}{2}, \qquad (2.3.4)$$

which is independent of the depression angle.

Error values, plotted for both the single and Janus cases, are shown in Figure 3. Note that the error is always negative in the Janus configuration, due to the asymmetry of the error of the single axis. At ±3° inclination the Janus error is -0.137%, where the single error is 5.09% for a negative inclination of 3° and -5.37% for a positive inclination of 3°. At the 7° inclination points the single system asymmetry is quite evident, the

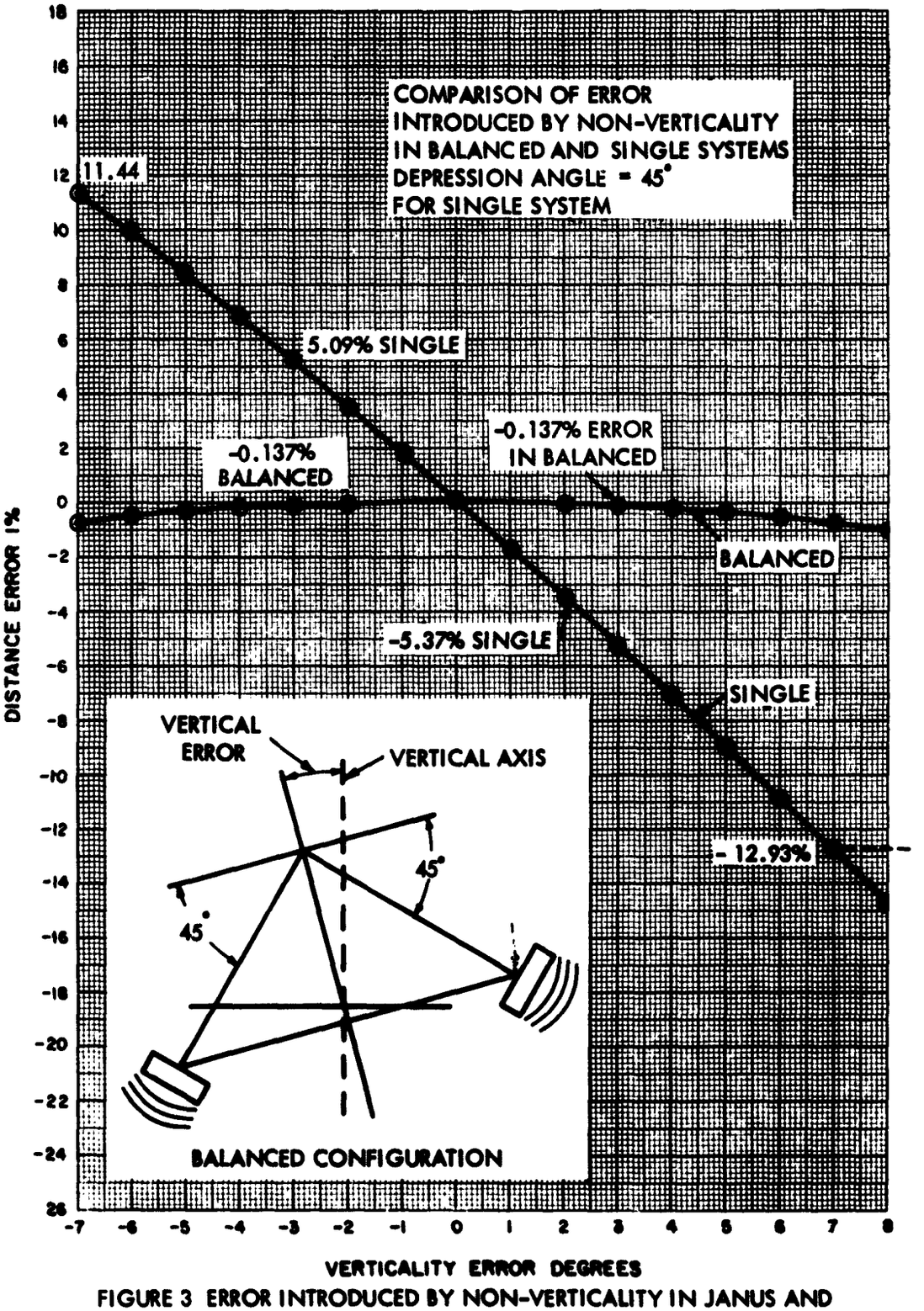

FIGURE 3 ERROR INTRODUCED BY NON-VERTICALITY IN JANUS AND SINGLE SYSTEMS

difference in magnitude of the errors caused by the positive and negative inclination being 1.5%. The error in the Janus configuration is about -0.75% for this 7° inclination. The superiority of the balanced arrangement in reducing indicated errors caused by array inclination is quite evident.

2.3.2 Pitch and Roll Errors

The effect of a symmetric motion of the array may be considered by allowing the angle θ to become a function of time, say $\theta(t) = \theta_m \sin \omega t$ where θ_m is the peak deviation, or amplitude, of the motion in the vertical plan and ω is the angular frequency of the motion. For the single-axis case the indicated shift may be integrated in time over a full cycle of the error angle θ, and the mean value of the indicated shift with the error angle may then be compared with the indicated shift when the error angle, θ,is zero.

If the single-axis Doppler shift given by Equation (2.3.1) is modified for $\delta = 45°$ and $\theta = \theta(t)$,

$$\nu_1 = \frac{K\sqrt{2}}{2} \left[\cos (\theta_m \sin \omega t) - \sin (\theta_m \sin \omega t) \right], \qquad (2.3.5)$$

This may be integrated over a full cycle of θ_m, which corresponds to a period of $\frac{2\pi}{\omega}$. The average shift over this interval is then

$$\frac{\sqrt{2}}{K} \overline{\nu_1} = \frac{\omega}{2\pi} \int_{-\frac{\pi}{\omega}}^{\frac{\pi}{\omega}} \left[\cos (\theta_m \sin \omega t) - \sin (\theta_m \sin \omega t)\right] dt \qquad (2.3.6)$$

which is

$$\frac{\sqrt{2}}{K} \overline{\nu_1} = J_o(\theta)$$

Comparing this with the shift obtained when $\theta_m = 0 = \theta$,

$$\nu_1 = \frac{\sqrt{2}K}{2},$$

the following is obtained for the percentage error:

$$\text{Error} = -100 \left[1 - J_o(\theta_m) \right] \%. \qquad (2.3.7)$$

The same sort of calculation may be carried out to illustrate the effects of pitch on a balanced system. If equation (2.3.2) is subtracted from equation (2.3.1).

$$\nu_1 - \nu_3 = 2K \cos\delta \cos\theta$$

and the steady shift is

$$\nu_1 - \nu_3 = 2K \cos\delta, \theta = 0. \tag{2.3.8}$$

The average over a full cycle of $\theta(t)$ is given by

$$\frac{\overline{\nu_1 - \nu_3}}{2K\cos\delta} = \frac{\omega}{2\pi} \int_{-\frac{\pi}{\omega}}^{\frac{\pi}{\omega}} \cos(\theta_m \sin\omega t)\, dt = J_o(\theta_m), \tag{2.3.9}$$

giving the same error for sinusoidal pitch as obtained for the single system,

$$\text{Error} = -100\,[\,1 - J_o(\theta_m)]\,\% . \tag{2.3.7}$$

The error values given by equation (2.3.7) are shown in Figure 4. On the basis of the tabulated values in Figure 4 it can be seen that some sort of compensation or stabilization is necessary if highly accurate navigation information is to be maintained for all weather conditions. It might be noted that the error produced by this condition always reduces the indicated velocity.

2.3.3 Sound Velocity Errors

Equation (2.1.3) indicates that the indicated velocity (Doppler shift) is dependent on the velocity of sound in the medium, C. If this velocity is not known and properly compensated, there will be a scaling error in the indicated velocity. For practical purposes, this error appears as a systematic error, probably nearly constant over a period of many days for any sheltered location. Since the major cause of change in the velocity of sound is due to temperature variations, the error due to variation in temperature has been computed and is illustrated along with the corresponding depression angles needed to keep the shift factor constant for a system with a nominal 45° depression angle.

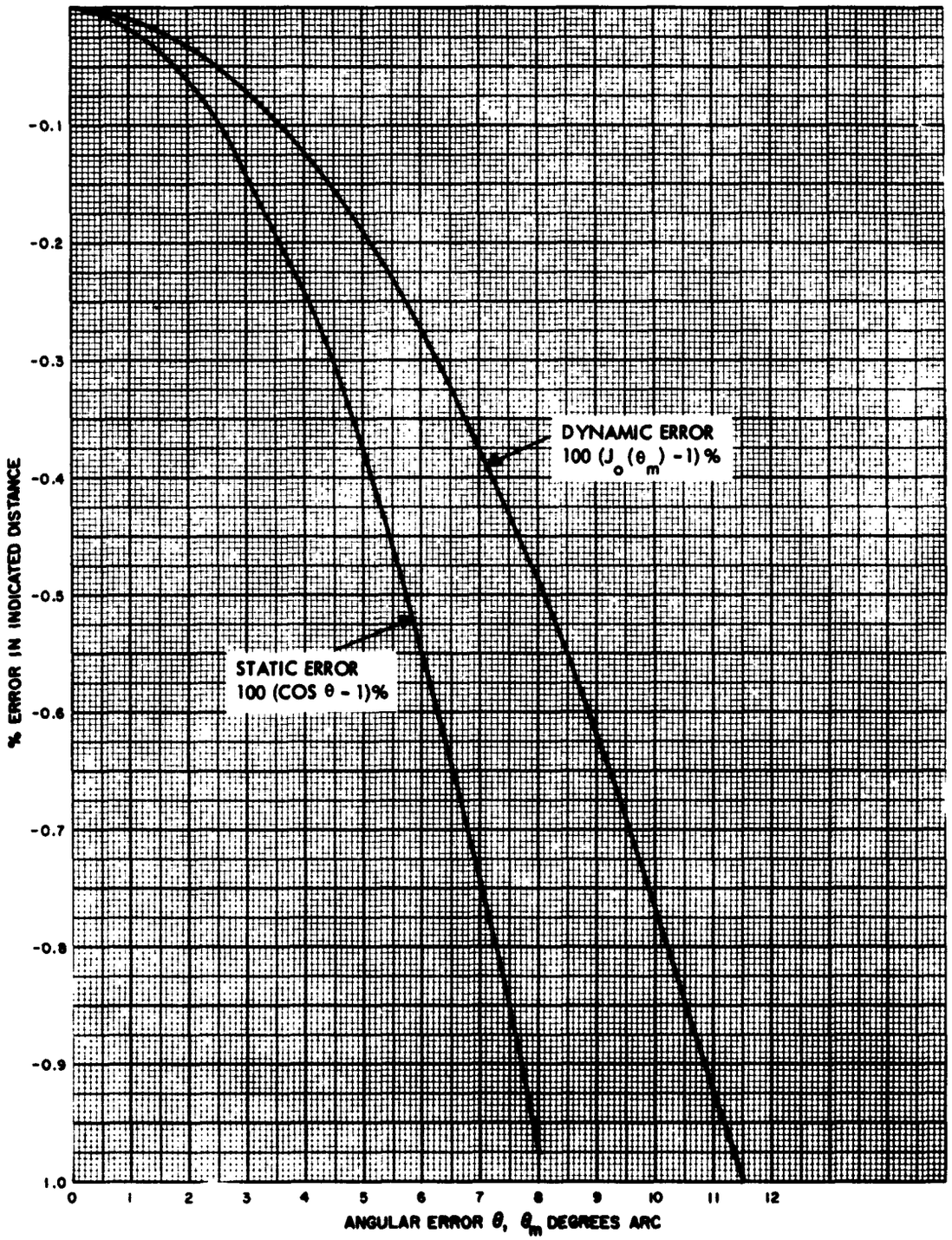

FIGURE 4 ERROR IN INDICATED DISTANCE TRAVELLED DUE TO ARRAY VERTICAL OFFSET

The velocity of sound may be approximated by Kuwahara's formula[2]:

$$C = 4422 + 11.25\,T - 0.045\,T^2 + 4.3(S-34) \qquad (2.3.10)$$

where

C = Velocity of sound, fps

T = Temperature, °F

S = Salinity, parts per thousand

and the simplified Doppler equation may be written as:

$$\nu = \frac{2\,V_S f \cos\delta}{4422 + 11.25\,T - 0.045\,T^2} \qquad (2.3.11)$$

if S is approximately 34 parts/1000 and the value of depth is small. If ν/V_S is fixed at some convenient value, say 100 cps/knot, then the desired depression angle, δ, may be computed, knowing f and T, as

$$\delta = \cos^{-1} \frac{\nu}{2V_S f}(4422 + 11.25\,T - 0.045\,T^2) \qquad (2.3.12)$$

Values of δ computed for a nominal δ of 45°, f of 210 kc and ν/V of 100 cps/knot = 59.25 cps/fps are shown in the upper portion of Figure 5. The lower curves of Figure 5 illustrate the velocity C versus water temperature as computed from equation (2.3.8). Computed values of indicated error are for an uncompensated situation. Fifty degrees Fahrenheit was chosen as a mid-point and the error was computed for every 10°F from 30° to 80°F using

$$100\,\frac{C_{50} - C_x}{C_{50}}\,\% = \text{Error} \qquad (2.3.13)$$

2.3.4 Linearity

As mentioned in Section 2.1 the linear Doppler equation, equation (2.1.3), has an error of approximation associated with it when compared with equation (2.1.2). The magnitude of this error may be easily determined using the relation

$$\text{Velocity Error} = 100\left(1 - \frac{1}{1 - \frac{V}{C}}\right)\,\% \qquad (2.3.14)$$

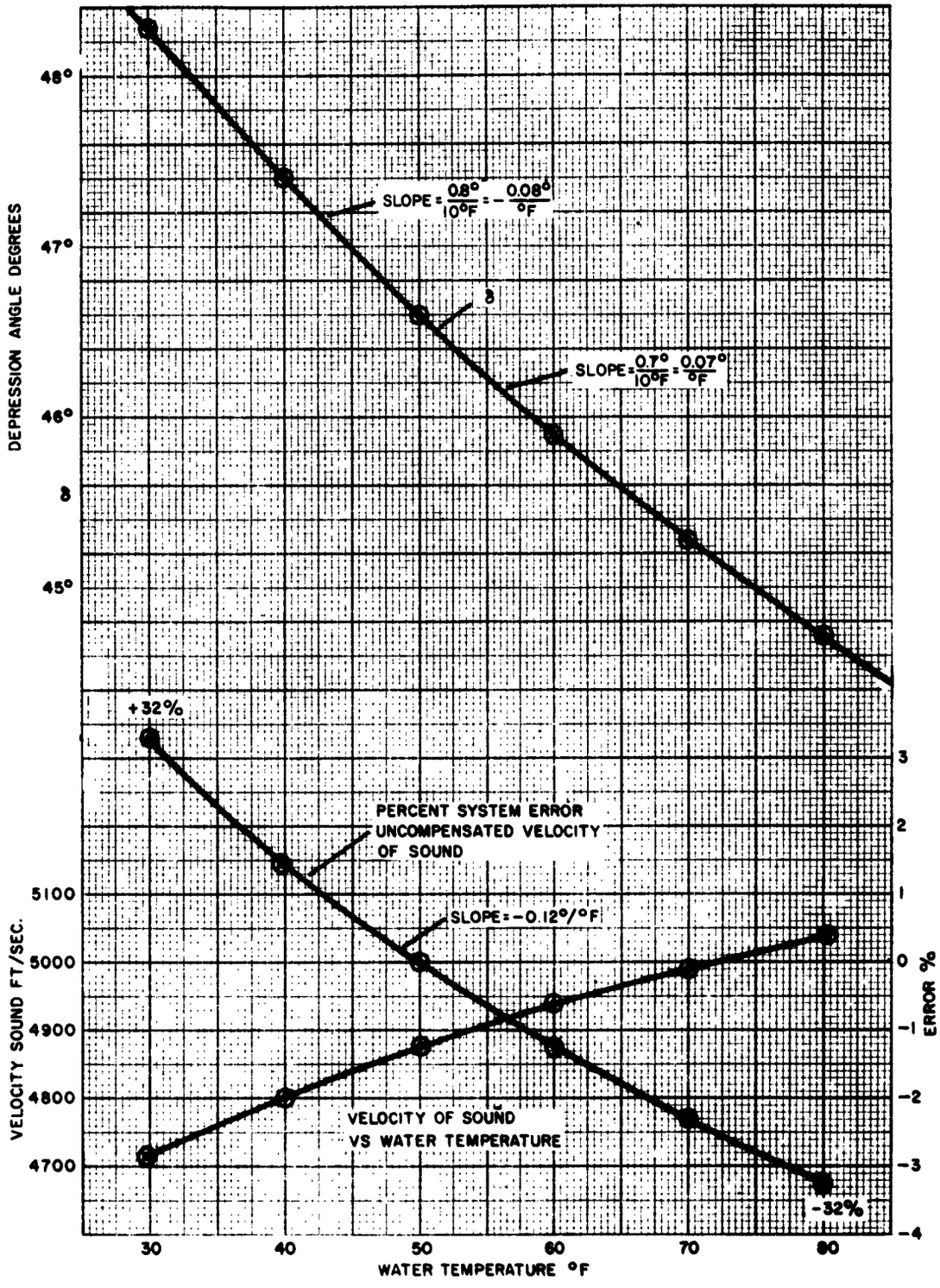

FIGURE 5 DOPPLER CORRECTION BY DEPRESSION ANGLE CONTROL

where V may assume either a positive or negative value according to whether V is in the direction of propagation (positive V) or against the direction of propagation (negative V). Using an assumed velocity of sound of 4800 ft/sec, the velocity error for a single axis system is tabulated below. It can be seen that this error is quite large for the higher ship velocities.

TABLE I - VELOCITY ERROR

Speed, Knots	Single System Velocity Error	Balanced System Velocity Error
1	0.035%	$1.24(10^{-6})\%$
10	0.352%	0.00124%
50	1.76%	0.031%

For the balanced system, the error due to this factor is small, the error being given by:

$$\text{Balanced Velocity Error} = 100\left(1 - \frac{1}{1 - \left(\frac{V}{C}\right)^2}\right)\%, \qquad (2.3.15)$$

values for which are tabulated in Table I also. These figures indicate that a balanced system is definitely advantageous on higher speed ships if no compensation for the velocity error is to be computed by the Doppler navigation device.

2.3.5 Compass Error

The primary error source in a stabilized, balanced Doppler Navigation system is compass error, or heading reference error. The magnitude of error introduced by the compass can be expressed in either the cross-track and track directions or in earth coordinates. Figure 6 indicates both errors.

The true coordinates as represented on the earth and on the navigator displays are the ordinate and abscissa of Figure 6. Line OA is the actual track, or velocity vector of length A. The coordinate system $N_r OE_r$ is the rotated coordinate system produced by the compass when an error angle E_c exists. Knowing that OA is the same length in either coordinate system, the errors may be quite simply derived from the compass error, E_c, and the course made good, C.

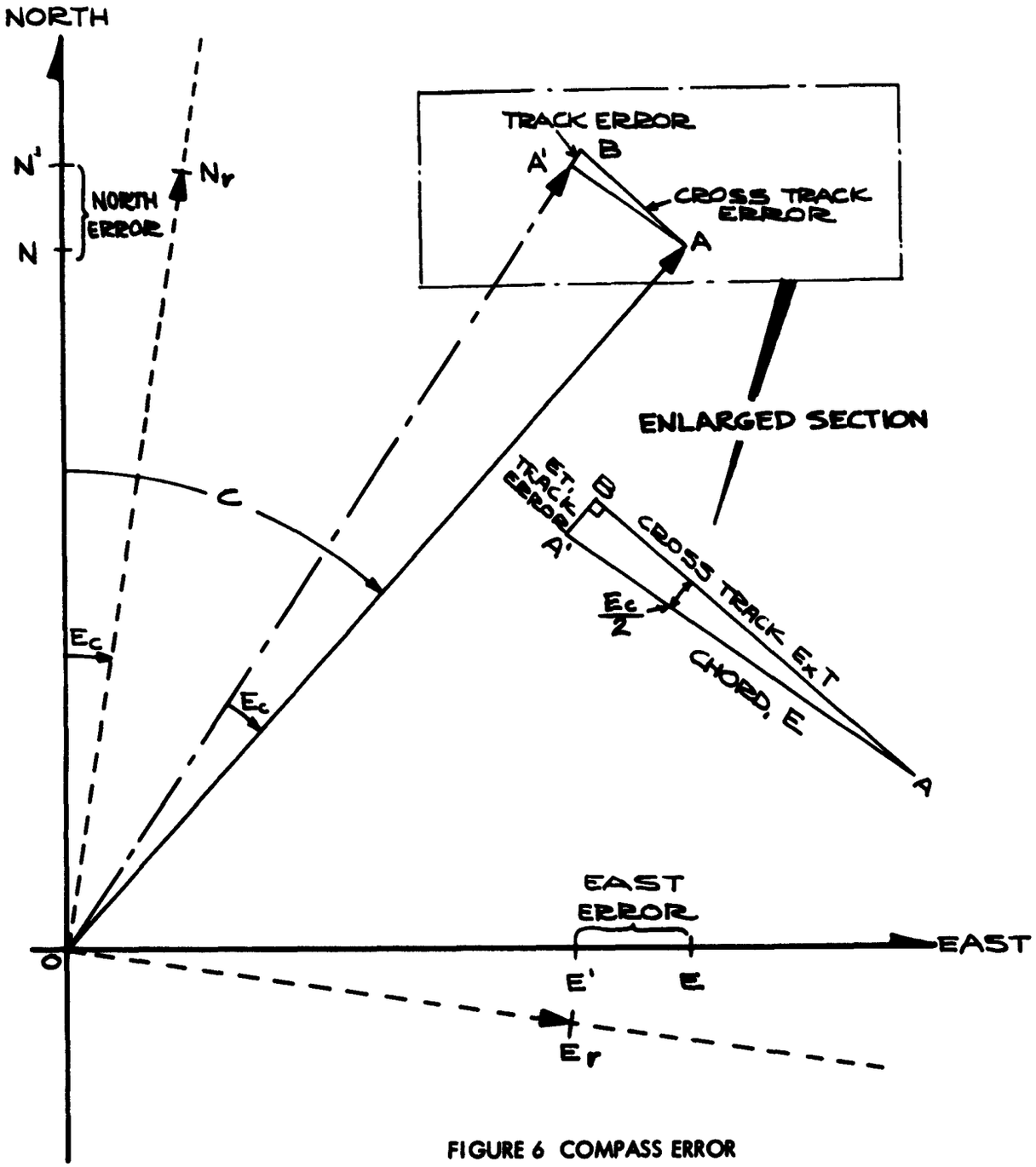

FIGURE 6 COMPASS ERROR

The northerly error is

$$E_N = ON' - ON = A \cos (C - E_c) - A \cos C \qquad (2.3.16)$$

and similarly the easterly error is

$$E_E = OE' - OE = A \sin (C - E_c) - A \sin C \qquad (2.3.17)$$

The normalized coordinate errors are not particularly useful since one or the other will be undefined if C is a multiple of $\pi/2$.

The cross-track error, E_{xT}, and the track error, E_T, are more useful in the normalized form, since they do not depend on the course, C. Since the indicated track OA' and the actual track OA form an isoceles triangle A'OA with vertex angle E_c, the line A'A is the chord of a circle of radius A defined by a central angle E_c. This chord, E, is

$$E = 2 A \sin \frac{E_c}{2}$$

in length and the triangle A'AB may be solved to give cross-track error

$$E_{xT} = E \cos \frac{E_c}{2} = 2A \sin \frac{E_c}{2} \cos \frac{E_c}{2} \qquad (2.3.18a)$$

or

$$\boxed{E_{xT} = A \sin E_c \approx A E_c} \qquad (2.3.18b)$$

The error along the track direction, E_T, is given by

$$E_T = -E \sin \frac{e}{2} = -2 A \sin^2 \frac{e}{2} \qquad (2.3.19a)$$

or

$$\boxed{E_T = -A (1 - \cos e) \approx \frac{A E_c^2}{2}} \qquad (2.3.19b)$$

which is much smaller than E_{xT}. Since E_{xT} is much larger than E_T and since the other error factors tend to act along the track if the direction of travel is close to a cardinal course, the compass error may be estimated if a traverse between two known points on a cardinal line is made. This fact has been utilized in calibrating the orientation of the experimental equipment in lieu of trying to boresight the transducers to the cardinal points, a task which could become quite complicated.

2.3.6 Spectral Contributions

The effect of finite aperture on the spectrum of back-scattered Doppler information has been the subject of many articles in the literature of Radar Doppler navigation. The bibliography in the last section of this report lists some pertinent documents on the general topic of Doppler navigation.

Berger[3] (page 109) gives the width of the Doppler spectrum as

$$\Delta\nu \simeq \frac{2V}{\ell} (\sin \delta_o) \Delta \delta_o$$

where $\Delta\delta$ = round trip half-power width of the beam pattern. For the system used in this study, allowing for the Janus scale factor, this gives

$$\Delta\nu = 200 V \Delta\delta , \qquad V \text{ in knots}$$

The half-power point of both receiving and transmitting units of the experimental system is about 6°, giving an effective round trip width of 4.25° = 0.074 radians, leading to an expected value of

$$\frac{\Delta\nu}{V} \approx 14.9 \frac{\text{cps}}{\text{knot}}$$

or 74 cps for 5 knots velocity.

A series of spectral measurements were taken with the transducers locked in the forward direction. The forward speed was held at 5 knots nominal and water depth varied from 20 to 160 feet. The analyzer used was the multiple-filter Rayspan with filter width of 8 cps and the sampling rate was 200 per second. The spectral width varied from 50 cps to 75 cps; the spectral width was estimated from 20 scans of the filter bank photographed on the face of an oscilloscope. Unfortunately, the camera has a light leak, rendering most of the photographs unsuitable for reproduction; Figure 7 is a tracing of the envelopes of spectra taken in 30 and 150 feet of water. Continuous observation of the spectra while traversing the range of depths did not indicate any apparent correlation between spectrum width and depth. Speed changes and rapid depth changes

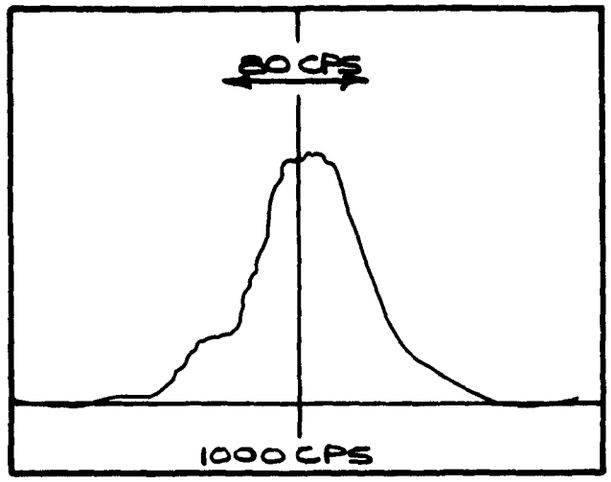

ENVELOPE OF MULTIPLE SCAN SPECTRA
DEPTH: 30 FEET
SPEED: 5 KNOTS NOMINAL

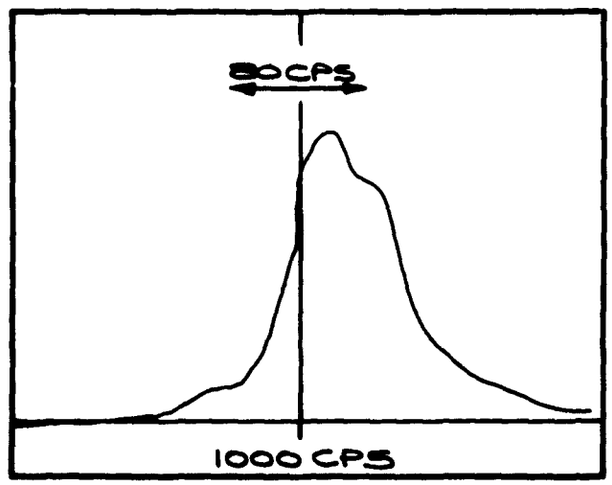

ENVELOPE OF MULTIPLE SCAN SPECTRA
DEPTH: 148 FEET
SPEED: 5 KNOTS NOMINAL

FIGURE 7 DOPPLER SPECTRA

did appear to widen the spectrum slightly but by no more than a factor of 1.5. This is a difficult point to interpret since the whole spectrum slides with speed changes, and depth changes would be expected to act differently on the fore and aft beams over the short sampling interval (5 milliseconds).

The observed spectra correspond very closely to the expected value of 74 cps for a velocity of 5 knots as computed previously. The expected contribution of spectrum width to system error may be computed by the method given by Berger[3] (pages 110, 111) and others.

Using Berger's results:

$$\frac{\sigma V}{V} = \frac{\sigma D}{D} \approx \frac{1}{\nu}\sqrt{\frac{\Delta\nu}{2T}} = \frac{1}{2}\frac{\sqrt{\sin\delta}}{\cos\delta}\frac{\sqrt{\Delta\delta}}{\sqrt{D}},$$

$\frac{\sigma V}{V}$ = normalized RMS velocity error,

$\frac{\sigma D}{D}$ = normalized RMS distance error,

$T = \frac{D}{V}$ = time to traverse distance D,

an expected value of $\sigma D/D$ for D = 1 mile may be computed using the following parameters:

$\delta = 45°$

$\ell = c/f = 0.02285$ ft.

$D = 6076.1$ ft.

$\Delta\delta = 0.074$ radians,

giving $\frac{\sigma D}{D} = 0.03\%$. The normalized value $\sigma D/D$ varies inversely with the square root of distance so that it can be seen that the expected error contribution of the spectral distribution of the Doppler signal soon becomes insignificant when compared with other error factors, such as the gyrocompass, which can be expected to contribute errors of the order of 0.1% due to composite errors in the data transmission system alone!

Note: Fried[4], (Appendix I) derives an expected Janus spectrum width, based on Berger's method, which is one-half the width of that given here. A performance factor is included which in later sections of Appendix I of this reference, is taken as 2, thus resulting in the equivalence of the two systems when considered in practice.

There have been predictions of observed errors of a larger magnitude than the above due to the shift in the apparent power center of the ensonified region of the bottom, due to the change in the exponent of the scattering law as regions of differing acoustic impedance are traversed[5]. Since no measurements of backscattering have been taken in this study, no conclusive data may be offered, but operation in both Narragansett and Chesapeake Bays have not produced errors which would seem to be ascribed to this source.

2.3.7 Conclusions Regarding Error

The major error factors acting on a sonar Doppler navigator are the heading and sound velocity errors. Of these two, the heading error is the most serious since the control of heading reference error is the most difficult to predict and/or correct. It is anticipated that the most effective method of controlling the sound velocity error will be accomplished through the use of a sound velocity controlled carrier frequency (constant wavelength transmission). To accomplish this, the tuned sense discriminators must be replaced by a discriminator that is not dependent on a fixed transmission frequency.

It has been noted experimentally that the relationship of equation (2.3.10) between sound velocity and depression angle is not exact, probably due to the fact that the energy is distributed in a finite beam width rather than in the infinitesimal beam assumed in the elementary analysis of the problem. Due to this fact, and considering the mechanical tolerances that would have to be held in compensating the sound velocity by changing the depression angle, this method of compensation appears to be impractical for anything but a laboratory device. The aforementioned constant wavelength transmission method would be recommended for an operational navigator.

The analysis outlined in the Second Interim Report on this project was completed and compared with experimental results, but in all instances, the actual performance was better than predicted.

This is undoubtedly due to the fact that continuous sinusoidal pitch and roll motions are an extreme worst case condition. The use of the data of Figure 4 gives adequate prediction of the errors to be expected due to imperfect stabilization when the average roll amplitude is taken as the independent variable. This is a much more economical method of prediction than solving the complete three-axis problem for each set of conditions involved.

In any case, the mean square error contributed by the gyrocompass will predominate in a stabilized, compass and sound velocity-compensated navigator. It may be stated then that for all practical purposes, shallow water Doppler navigation accuracy is at present limited by the accuracy of available heading references.

3.0 EXPERIMENTAL RESULTS

This section describes the results obtained with three different configurations of equipment. The errors of closure are presented for ninety-five runs, of which the majority were 2.7 miles in length. Scaling errors are not considered because of the lack of exact data on shore positions and the fact that sound-velocity calibration and compensation were not accomplished on a continuous basis. Demonstration of closure capability indicates the attainable performance when scaling parameters are properly adjusted. The operating depths on these cases ranged from 2 to 30 fathoms.

3.1 Case I - Unbalanced System

Fifty-eight runs were made using an unbalanced, unstabilized navigator. No compass compensation was applied. This corresponds to what would now be considered a sub-marginal operational system. The following histograms show the distribution of errors (Figure 8). The statistics computed for this series are:

Mean North-South Error	0.13% North
Standard Deviation, North-South	0.95%
Mean East-West Error	0.6% East
Standard Deviation, East-West	3.6%

The existence of the distinct correlation between North and East errors may be attributed to the gyrocompass since the starting transient was to the northwest, which would be expected to produce a westerly compass error and an easterly indicated error on the leg of the run which was predominately North-South, and a northerly error on the leg which was predominately West-East. Although it was not detected at this time, later tests showed that rough water caused a severe distortion of Doppler signal when running at speeds above 5 knots. This effect was correlated with the appearance of large numbers of air bubbles in the sea chest of the training gear, thus pointing toward the conclusion that

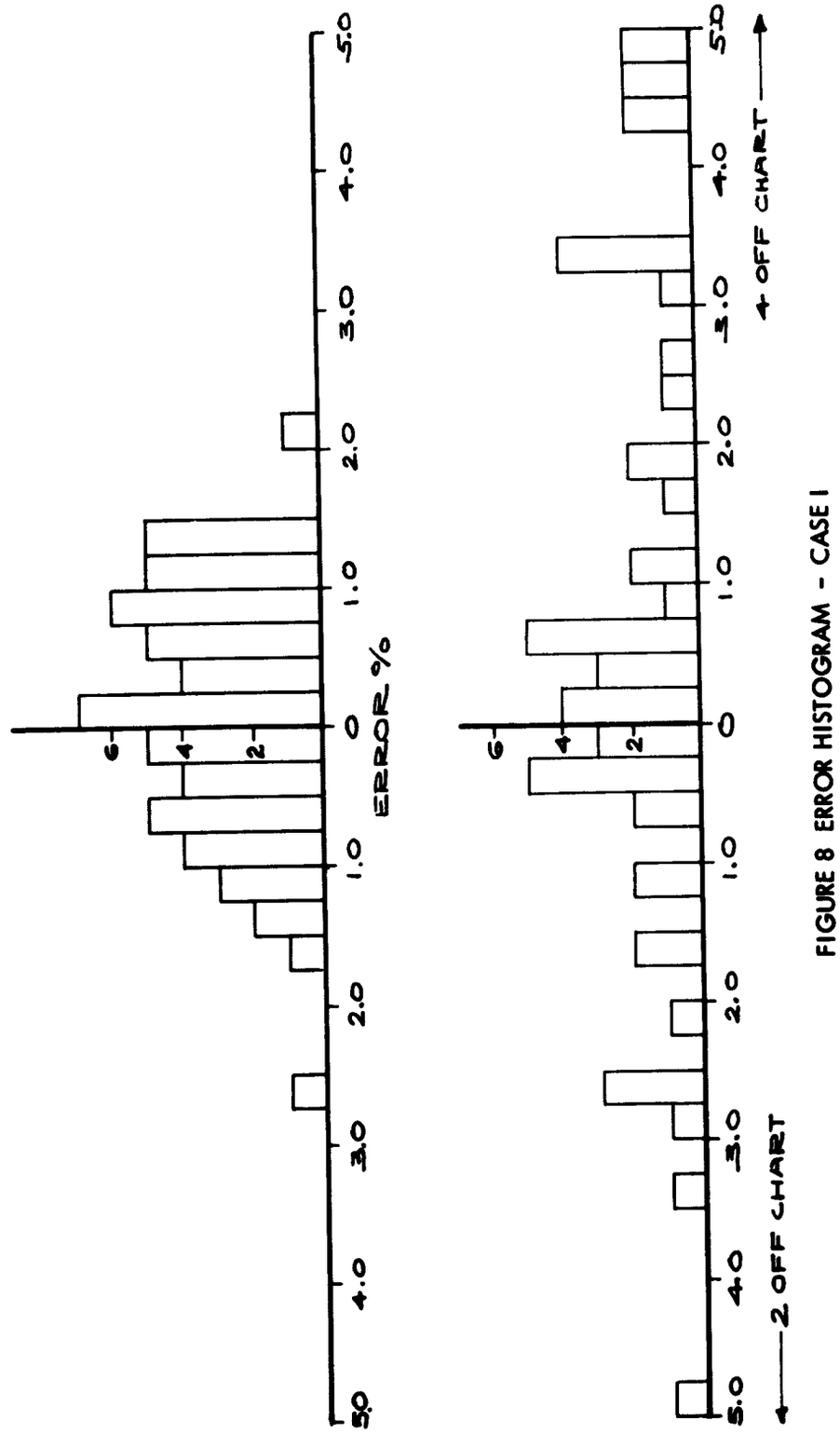

FIGURE 8 ERROR HISTOGRAM - CASE I

bubbles from the bow wave were being introduced into the acoustic path of the navigator. This may have been a contributing factor toward the extreme peak errors noted in Cases I, II and III, but since this effect was not noticed until after the data were taken, the data were not changed.

3.2 Case II - Balanced System

The acoustic configuration was modified to the Janus form (axes in all cardinal directions) to eliminate possible errors due to depth variations. The Mark 19 gyrocompass was installed without velocity correction and the acoustic and electronic equipment was installed without physical stabilization of the transducer array.

At the first glance, the results were rather disappointing, as can be seen in the histogram (Figure 9). The errors were not as large on the whole as before and the variability was reduced, but the design goal of 0.5% was not attained. A consistency in the amount and direction of error had at least been attained.

The statistics for this case were:

Mean error, North-South	1.52%
Standard Deviation	1.28%
Mean error, East-West	1.05%
Standard Deviation	0.47%

Since the number of samples (17) was small, the population deviation has been computed from the chi-square distribution at the 95% level as

$$0.183\% \leq \sigma NS \leq 0.765\%$$

$$0.067\% < \sigma NW < 0.28\%$$

3.3 Case III - Velocity-Corrected and Stabilized Balanced System

Velocity correction for the gyrocompass was installed in May 1962 and three runs were made with the digital display disassembled, thus the actual errors of these runs were not known, but the charted runs showed a great reduction in the tendency of generation of errors only northward and eastward. The stabilizer for the transducer array was then installed, bringing the equipment to its present state and the errors shown in Figure 10 have been noted.

The statistics for this case were:

Mean error - North-South	0.078%
Standard Deviation North-South	0.072%
Mean error East-West	0.064%
Standard Deviation East-West	0.096%

As for Case II, the population deviation has been computed, on the basis of the small sample, to be:

$$0.0098\% < \sigma \text{ NS} < 0.036\%$$

$$0.054\% < \sigma \text{ EW} < 0.198\%.$$

The average error is noticeably less and the variability has been reduced by a significant amount. Certain difficulties are still being experienced with the gyrocompass in that rapid maneuvering produces accelerations which result in heading errors. Extremely tight turns at 7 or 8 knots seem invariably to cause closure errors.

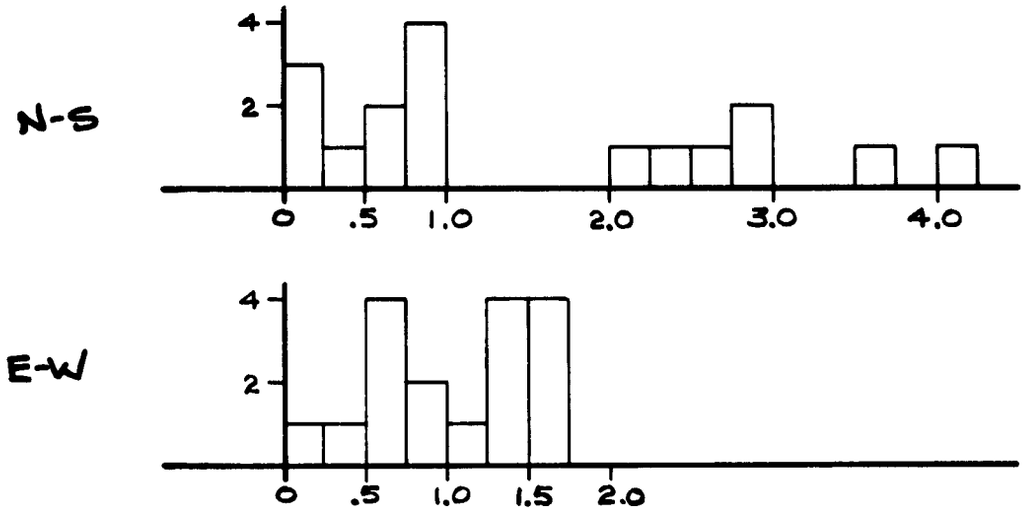

FIGURE 9 ERROR HISTOGRAM - CASE II

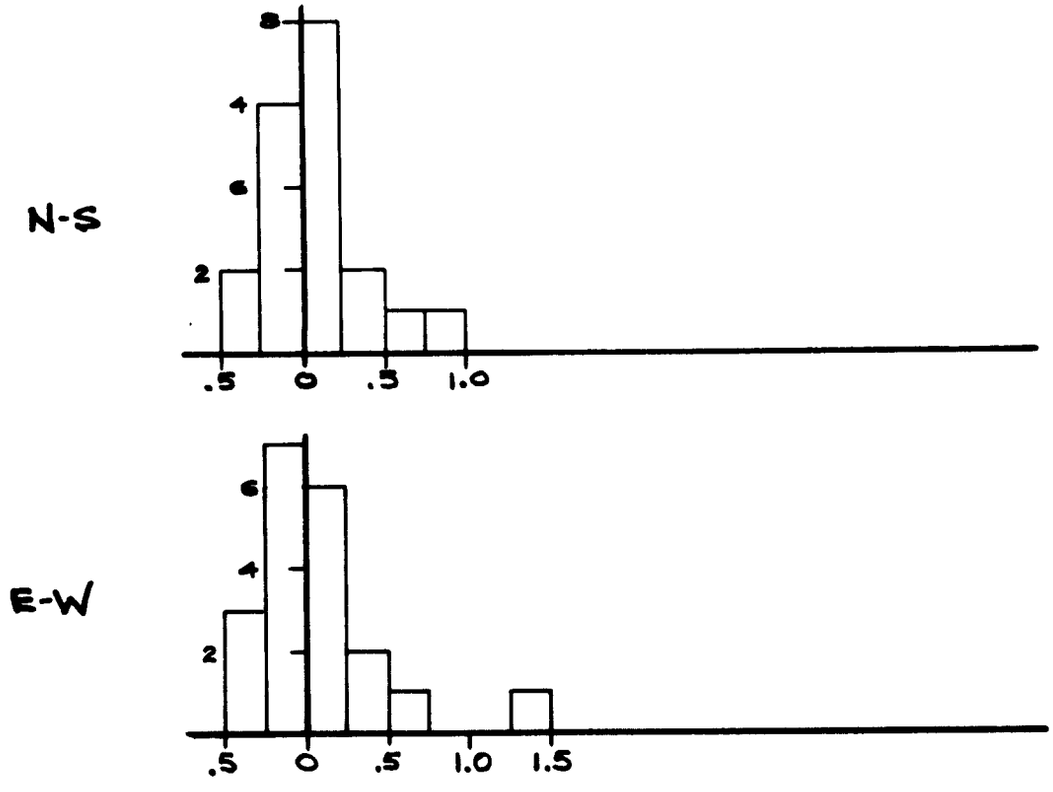

FIGURE 10 ERROR HISTOGRAM - CASE III

4.0 EXPERIMENTAL EQUIPMENT

The following paragraphs describe the equipment; descriptions of some parts of the equipment were presented in the Third Interim Report of this study.

4.1 Acoustic Equipment

4.1.1 Transmitting Transducers

The active elements of the transmitting transducers are circular disks of poled barium titanate ceramic approximately four inches in diameter and approximately one-half inch thick. The disks operate in the thickness mode of a frequency of 210 kilocycles per second. Being over 14 wave lengths in diameter, the directivity index is 33 dB. The beam width at the 3 dB down points is less than 4.5 degrees.

Each disk is power-factor corrected by a toroidal core transformer. The primary impedance of the transformer is approximately 32 ohms; the four transmitting transducers are paralleled to obtain an 8-ohm load impedance for the transmitter.

The transmitting efficiency of these units is in excess of 50 percent. Each unit receives two watts of electrical power, resulting in an acoustic output power in excess of one watt for each unit.

The transmitting ceramic disk is housed in a cylindrical aluminum cup, which is anodized for corrosion protection. Acoustic isolation material of cork in a neoprene binder (corprene) is used on the side and back faces of the disk. The disk is supported in the housing on blocks of corprene; the housing is filled with an elasticized epoxy compound to provide a waterproof assembly. The electrical cable is led through a threaded stud which serves as the mounting member, and is located on the bottom of the aluminum cup.

The four matching transformers for the transmitters are located in a separate aluminum housing and watertightness is assured by a gasketed cover plate and silicone rubber encapsulation of the transformers.

4.1.2 Receiving Transducers

The active elements of the receiving transducers are identical to those of the transmitting transducers. Unlike the transmitting units, however, the receiving units employ a novel mounting of the active element.

The difference in transducer construction between transmitting and receiving units arises from the need to locate the receiving preamplifiers as close to the receiving transducer as possible. For this reason, the preamplifiers are placed in the transducer housing. The housing is basically the same as the transmitter housing, being an anodized aluminum cup. Electrical cable is led through the same type of threaded stud on the bottom of the cup. The ceramic disk is not embedded in potting compound in the cup as in the transmitting units; instead, the receiving ceramic disk is bonded to a thin anodized aluminum dome. The periphery of the aluminum dome fits into a groove on the upper edge of the cup, the groove then being filled and sealed with lead. The resulting transducer assembly leaves sufficient space in the interior of the cup to accommodate the preamplifier. The preamplifier, which provides 45 dB of voltage gain, is encapsulated for physical protection.

4.2 Mechanical Equipment

4.2.1 Transducer Array Fixture

The transducer array fixture has four purposes:

a) to locate the four transmitting-receiving transducer pairs in two mutually perpendicular vertical planes.

b) to locate each receiving transducer at the same depression angle.

c) to provide for adjustment of the depression angle for temperature compensation.

d) to provide maximum acoustic isolation between any one receiving transducer and all other transducers, but especially the associated transmitting transducer.

Since the array fixture is not shielded by a dome, the shape of the fixture must minimize water drag forces. The shape chosen to fulfill all of these requirements is roughly that of an hourglass. The lower inverted cone holds the four transmitting transducers, while the upper inverted cone holds the four receiving transducers. Joining the two inverted cones is an upright cone. The cones position the transducers while the placement of the receiver cone over the transmitter cone provides isolation of the transmitter beam from the receiver beam.

The fixture is hollow; each transducer is located inside looking out through a circular hole in the cone face. The transducers are mounted on plates pivoted on a horizontal axis, the pivot points being adjustable so that the transducers can be aligned to look in mutually perpendicular vertical planes. The receivers are locked together, with an adjusting mechanism to provide adjustment of the depression angle. Adjustment for temperature compensation is affected from topside by means of push-pull flexible cables attached to the receiver linkage. As the cables are positioned by a topside screw adjustment, the linkage produces a corresponding rotation of the receiving transducers about their horizontal pivot axis.

Acoustic isolation between transducers is effected, first, by the separation of transmitting and receiving cones as mentioned above and, second, by generous use of isolation material (Corprene) to break any acoustic propagation path other than the exterior water path. Each transducer is covered by corprene 1/4-inch thick on the transducer case to virtually eliminate transmission or reception of acoustic energy through the case. Corprene was also applied to the exterior face of the upright cone to minimize spurious transmissions through the cone into the receiver beams.

The fixture is made of aluminum plate anodized for corrosion protection. At various stages in the program the fixture was removed from the water for modifications. At each removal several man-days were spent removing marine growth from the head and

especially the transducer faces. Corrosion of the head became noticeable after several months. To eliminate these problems, an antifouling, anti-corrosion protective coating of a Raytheon proprietary material was applied. After a six-month immersion following the application of this coating, no fouling or further corrosion was noted.

4.2.2 Azimuth Drive System

The transducer array fixture is rotated by the azimuth drive system. The fixture is fixed to a vertical shaft protruding through a sea chest in the hull. (Interposed between the shaft and the fixture is the stabilization system described in the next section.) The shaft rotation is controlled by a servomechanism whose reference is a Mark 19 gyrocompass. The shaft is rotated so as to maintain the north-south transducer axis in the north-south direction, as indicated by the gyrocompass.

The control or error signal for the servomechanism is produced by comparing the shaft position with the indicated north of the gyrocompass. The comparison is done in a two-speed (1 : 1, 36 : 1) synchro transformer mechanism geared to the shaft. The error signal is amplified to drive a motor geared to the training shaft to null the error signal.

4.2.3 Stabilization System

Interposed between the training shaft and the transducer array fixture is a stabilization system. The purpose of the stabilization system is to maintain the fixture's axis vertical.

Basically the system consists of two horizontal plates joined by a flexible vertical link, which is a ball joint inside a bellows. This construction was used for the vertical link to achieve a constant velocity joint between the training shaft axis and the transducer array fixture axis. The attitude of the lower plate fixed to the top of the array fixture is

sensed by a pair of electrolytic levels mounted at right angles, being aligned with the North-South and East-West axes of the array fixture. A deviation from the vertical produces an electrical signal from the levels. This signal is amplified and applied to electro-hydraulic servo valves which then apply hydraulic pressure to pairs of hydraulic cylinders. Actuation of the cylinders produces the necessary corrective motion to bring the lower plate, and thus the array fixture, to vertical. The servo valves and the hydraulic power source are fixed to the top of the training shaft.

Although the purpose of the stabilization system is to maintain the array vertical independent of vessel rolling and pitching, the stabilization system only stabilizes for small vessel motions. For larger motions, the system will but attenuate the motions of the array. The fault of the system lies with the electrolytic levels used to sense deviations from vertical. The levels are subject to shifting of the liquid under acceleration. The resulting system tends to oscillate at a frequency in the region of the frequency vessel motion. The average vertical of the array fixture is maintained, however, under the light sea conditions normally encountered in the test waters, the stabilization system performing satisfactorily.

4.3 Display

4.3.1 Plotter

The vessel's track is displayed on standard navigational charts by an X-Y plotter. The plotter employs two rods at right angles step-driven by rotary solenoids driving ball nuts along lead screws. A marking pen is positioned by the intersection of the two rods. Thus as the rods are driven in the X and Y directions in correspondence to the input pulses in those directions, the pen draws the track of the vessel.

Each input pulse to the rotary solenoid produces a rod step motion of 0.0073 inches, corresponding to a travel of 0.001 nautical miles on a chart scale of 1:10,000. The direction and scale factors are set by the discriminator and scaling circuits as indicated previously.

4.3.2 Counters

The distance travelled is displayed by four counters, one counter for each cardinal direction. These counters are fed the same pulses as the plotter but are mechanically independent. The counters serve to record the total distance travelled in each cardinal direction.

4.3.3 Speed Meters

The North-South and East-West velocity of the vessel is displayed by two speed meters. The direction of the vessel's velocity, whether North or South, is indicated by lights activated by the discriminator.

4.3.4 Vessel Heading

The vessel's heading is indicated by a gyro repeater unit.

4.4 Electronics

The electronic portion of the navigator has been described in detail in the Third Interim Report of this study and with one exception remains the same.

In order to compensate for velocity effects on the gyrocompass, a compass speed converter unit has been added to the navigator.

This unit converts the Doppler frequencies, North-South and East-West, into 400-cycle signals scaled to provide the proper control to the compass. The Doppler pulse information drives a magnetic pulse conditioner, the output of which is rectified, integrated and chopped to 400-cycle pulses. These are amplified and filtered to provide the proper amplitude and waveform for the compass. The phase of the 400-cycle signal is controlled by switching the chopper drive phase with the direction sense signal from the discriminators. The scale factor has been set at 0.75 volts per knot which is fed into the

Mark 19 compass, replacing the output of the compass speed resolver. Since the speed information is already resolved into North and East components and is bottom-referenced, the drift setting and speed resolver of the compass are not needed. Since the speed deviation angle in the vicinity of Newport, R.I., amounts to 0.08 degrees per North knot, the error induced by uncompensated speed is significant. The reduction in error between the second and third series of runs mentioned before is thought to have been effected, in good part, by the addition of this speed compensation.

4.5 Significant Equipment Parameters Summarized

The following is a tabulation of the significant parameters of the experimental equipment.

4.5.1 Electrical

Operating Frequency	210 Kilocycles/second
Transmission Mode	CW
Electrical Power Output	8 watts at 210 kc
Hydrophone Preamplifiers	
Gain	45 dB
Bandwidth	4 kc to clipper inputs
Clipper Amplifiers	
Gain to clip	112 dB
Bandwidth	80 kc
Clip Level	-100 dB
Output Level	2.5 V RMS (Saturated)
Mixer Bandwidth	80 kc
Low Pass Filter Bandwidth	1500 cps
Doppler Voltage Level	2 V RMS

Scaling Circuits		
Scale Factors	15 (Test) 360, 1:5,000 720, 1:10,000 1440, 1:20,000 2880, 1:40,000	Scales
Discriminator		
Hysteresis	2 cps	
Band Limits	±2 kc	
Compass Speed Converter		
Pulse Input	4 V	
Pulse Input Rate	0 - 2 kc	
Output	400 cps sine wave	
Output Scale Factor	7.5 mV/cps	
Linearity	<1%	
Null	<100 mV	
Power Inputs		
115-V 60-cps Single phase	≈ 750 W	
115-V 400-cps Single phase	10W (chopper drive)	
440-V 60-cps 3-Phase	1.5 H.P. motor load	
Level Control Amplifiers		
Input	60-cps signal from levels	
Input Level Gradient	≈ 1 Volt/degree	
Magamp Output Saturation Level	≈ 8 Volts dc into 1000 ohms servo valve	
Gain	10 (variable)	
Azimuth Control Amplifier		
Input Signal Source	23CT6 synchro (1 & 36 speed)	
Input Signal Gradient	≈ 1 volt/degree	
Input Saturation Level	≈ 2.5 V RMS	
Output Level	2 Amps dc (max), 300 V	

4.5.2 Acoustic Parameters

Transducer Material	Barium Titanate Disk
Diameter	4 inches
Directivity	~30 dB actual
Beamwidth (3 dB)	6 degrees
Side Lobes (first)	18 - 22 dB down
Efficiency	~ 50%
Power Output	1 watt/projector
Receiving Sensitivity	~ -83 dB vs 1 volt//μbar at 1 yard

5.0 CONCLUSIONS

The research and experimental verification thereof have proven that a suitably configured Doppler navigation system can provide extremely accurate, bottom-referenced, speed and position information. In the course of this study, certain other areas of uncertainty have become evident although they in no way should cast doubt upon the validity of the work already accomplished. These areas are: 1) The need for accurately determined volume reverberation strengths and 2) A more accurate description of the backscattering process. References 1, 6 and 7 discuss these problems.

REFERENCES

1. Sims, D.S., "CW Reverberation as a Function of Frequency", Journal of Underwater Acoustics, Vol. 6, 2, 1956, (Confidential)

2. Horton, J.W., Fundamentals of Sonar, U.S. Naval Institute

3. Berger, F.B., "The Nature of Doppler Velocity Measurements", IRE Transactions, ANE-4, 3, 1957

4. Fried, E.R., "Doppler Navigation Systems and Practice", AD118271

5. Potter, E.V., "Frequency Spectrum and Shape of Bottom Echoes as Observed with a Moving Transducer", Journal of Underwater Acoustics, Vol.7, 3, 1957 (Confidential)

6. Mackenzie, K.V., "Reflection of Sound from Coastal Bottoms", Journal of the Acoustical Society of America, Vol. 32, 2, 1960

7. Urick, R.J., "The Backscattering of Sound from a Harbor Bottom", Journal of the Acoustical Society of America, Vol. 26, 2, 1954

Other references of interest may be found listed in the IRE Transactions, ANE-4, both in the September and December issues of 1957.

DISTRIBUTION LIST

AGENCIES	NO. OF COPIES
Office of Naval Research Department of the Navy Washington 25, D.C.	
ATTN: Code 463	2
Code 466	1
Code 406	1
Chief of Naval Operations Department of the Navy Washington 25, D.C.	
ATTN: Op-03	1
Op-323	1
Op-07	1
Op-07T	1
Op-715	1
Chief, Bureau of Naval Weapons (Code RUME) Department of the Navy Washington 25, D.C.	1
Chief, Bureau of Ships Department of the Navy Washington 25, D.C.	
ATTN: Code 362	1
Code 364	1
Code 631	1
Code 689A	1
Director U.S. Naval Research Laboratory Department of the Navy Washington 25, D.C.	
ATTN: Tech. Information Div	6
Commanding Officer Office of Naval Research Branch Office 495 Summer Street Boston, Massachusetts 02110	1
Commanding Officer Office of Naval Research Branch Office Box 39, Navy 100, F.P.O, New York	1
Commanding Officer and Director U.S. Navy Mine Defense Lab Panama City, Florida	1
Mine Advisory Committee National Academy of Sciences National Research Council 2101 Constitution Avenue, N.W. Washington 25, D.C.	1
Superintendent U.S. Naval Postgraduate School Monterey, California	1
Commander, Mine Force U.S. Atlantic Fleet U.S. Naval Minecraft Base Charleston, South Carolina	1
Commander, Mine Force U.S. Pacific Fleet c/o Fleet Post Office San Francisco, California	1
Commanding Officer Defense Documentation Ctr Cameron Station, Building 5 5010 Duke Street Alexandria, Virginia	20